

# Nanoscale

Accepted Manuscript



This is an *Accepted Manuscript*, which has been through the Royal Society of Chemistry peer review process and has been accepted for publication.

*Accepted Manuscripts* are published online shortly after acceptance, before technical editing, formatting and proof reading. Using this free service, authors can make their results available to the community, in citable form, before we publish the edited article. We will replace this *Accepted Manuscript* with the edited and formatted *Advance Article* as soon as it is available.

You can find more information about *Accepted Manuscripts* in the [Information for Authors](#).

Please note that technical editing may introduce minor changes to the text and/or graphics, which may alter content. The journal's standard [Terms & Conditions](#) and the [Ethical guidelines](#) still apply. In no event shall the Royal Society of Chemistry be held responsible for any errors or omissions in this *Accepted Manuscript* or any consequences arising from the use of any information it contains.

**Article type: Communication**

**Binary  $A_xB_{1-x}$  ionic alkaline pseudocapacitor system involving manganese, iron, cobalt, and nickel: formation of electroactive colloids via in-situ electric field assisted coprecipitation**

*Kunfeng Chen<sup>1</sup>, Shu Yin<sup>2,\*</sup> and Dongfeng Xue<sup>1,\*</sup>*

<sup>1</sup>State Key Laboratory of Rare Earth Resource Utilization, Changchun Institute of Applied Chemistry, Chinese Academy of Sciences, Changchun 130022, China

<sup>2</sup>Institute of Multidisciplinary Research for Advanced Materials, Tohoku University, 2-1-1 Katahira, Aoba-ku, Sendai 980-8577, Japan

\*E-mail: shuyin@tagen.tohoku.ac.jp; dongfeng@ciac.ac.cn

A new “combinatorial transition-metal cation pseudocapacitor” was demonstrated by designing combinatorial transition-metal cation pseudocapacitors with binary  $A_xB_{1-x}$  salt electrodes involving manganese, iron, cobalt, and nickel cations in alkaline aqueous electrolyte. Binary multi-valence cations were crystallized in colloid through an in-situ coprecipitation under electric field. These electroactive colloids absorbed by carbon black and PVDF matrix are highly redox-reactive with high specific capacitance values, where the specific electrode configuration can create short ion diffusion paths to enable the fast and reversible Faradaic reactions. This work shows promise for finding high-performance electrical energy storage systems via designing the colloidal state of electroactive cations. Multiple redox cations in colloid can show high redox activities, making them more suitable for potential application in pseudocapacitor systems.

Keywords: pseudocapacitor, transition metal cation, colloid, coprecipitation, binary salt

Breakthroughs in battery or supercapacitor science and technology are highly demanded to meet various needs of modern society and many concerns of environment and energy security. Supercapacitors can provide higher energy density by orders of magnitude than dielectric capacitors, greater power density, and longer cycling ability than rechargeable batteries.<sup>1,2</sup> The capacitance of supercapacitors mainly originates from surface charge separation at the electrode/electrolyte interface and surface Faradaic redox reactions at the surface of electrode materials, which respectively correspond to electrical double-layered capacitors and pseudocapacitors.<sup>1</sup> As typical pseudocapacitance materials, transition metal oxides or conductive polymers show much higher specific capacitance values than carbon-based materials as the electrical double-layered capacitors. Because that surface charge storage is not dependant on the ionic diffusion within the crystal lattice of electrode materials, supercapacitors possess fast charge/discharge rates (i.e., high power density), but lower energy density compared to batteries.<sup>3,4</sup> Facing this challenge, many efforts have been made to improve their energy density values.<sup>5-7</sup> The energy density ( $E$ ) of any supercapacitor is a function of both specific capacitance ( $C$ ) and voltage ( $V$ ),  $E = 0.5CV^2$ , therefore, a boost in energy density can be achieved by increasing the capacitance or voltage window.<sup>5</sup>

In particular, electrode materials that exploit physical adsorption and redox reactions of electrolyte ions are foreseen to bridge the performance disparity between batteries with high energy density and capacitors with high power density.<sup>8</sup> The application of nanostructured materials with bespoke morphologies and properties to supercapacitors has been intensively studied in order to obtain enhanced energy density without compromising their inherent high power density and excellent cyclability.<sup>8-12</sup> To facilitate rapid diffusion of active cations during the charging/discharging processes in supercapacitors, two solutions have been found:<sup>3,4</sup> (1) the large contact area between current collector and active material can significantly shorten the electron transportation path length and (2) decorating active nanomaterials onto nanostructured current collectors leads to the increase in number of

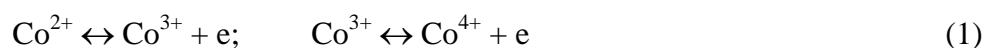
electrochemically active sites for the redox reaction. Therefore, the composite electrode materials were found with the aim to utilize more active species.<sup>13,14</sup> Recently, it is reported that the mixed-valence manganese oxide film including  $\text{Mn}^{4+}$  and  $\text{Mn}^{3+}$  exhibited anomalously high specific capacitance,<sup>15</sup> which prove that the multiple electroactive cations in the same electrode can increase the specific capacitance for pseudocapacitor. An efficient strategy to enhance the electrochemical performance of metal oxide/hydroxide pseudocapacitive materials is incorporating one or two metal ions into them to form multi-metal compounds, such as Ni-Co, Mn-Co and Ni-Zn-Co oxides or hydroxides, which can introduce abundant structural defects and ensure fast redox reactions.<sup>16-18</sup> Here, we introduce a new combinatorial transition-metal cation pseudocapacitor, which shows huge promise for finding high performance electrical energy storage systems by coupling the contribution of electroactive cations. This binary  $\text{A}_x\text{B}_{1-x}$  ionic alkaline pseudocapacitor is expected to benefit from the major advantages of multiple redox cations, which can provide multiple redox sites to enhance electrochemical performances. Multiple redox cations coupled with their high redox activities can make them more suitable for their extensive applications in pseudocapacitor systems.

The commercial  $\text{MnCl}_2 \cdot 4\text{H}_2\text{O}$ ,  $\text{FeCl}_3 \cdot 6\text{H}_2\text{O}$ ,  $\text{CoCl}_2 \cdot 6\text{H}_2\text{O}$ ,  $\text{NiCl}_2 \cdot 6\text{H}_2\text{O}$  salts were directly used without further purification. The binary  $\text{A}_x\text{B}_{1-x}$  salts electrodes consist of two kinds of salts (A and B = Mn, Fe, Co, Ni) with different molecular ratios ( $0 \leq x \leq 1$ ), which were directly used as work electrode in electrochemical measurement. Cyclic voltammetry (CV), and galvanostatic charge-discharge measurements were measured in 2 M KOH electrolytes at designed potential range, scan rate and current density. Scheme 1 shows the in situ formation of electroactive media under electric field and the charge storage mechanism of the binary  $\text{A}_x\text{B}_{1-x}$  cation pseudocapacitor. Firstly, slurry-coating manufacturing was used to prepare binary  $\text{A}_x\text{B}_{1-x}$  electrode. Two kinds of water-soluble inorganic salts with different molecular ratios were mixed with carbon black and binder to form the slurry, which was spread onto Ni

foam current collector for the fabrication of electrode (Scheme 1a and b). Then, the binary  $A_xB_{1-x}$  electrode was measured in KOH electrolyte (Scheme 1c). After the as-prepared electrode was immersed into KOH electrolyte, CV measurements were performed immediately, meaning that external electric field was applied upon binary salt electrode at this time. In this CV measurement process, various chemical reactions, electrochemical reactions, and Faradaic redox reactions were simultaneously occurred. Binary transition metal salts immediately transform into hydroxides or metal oxides colloids by the electric field assisted chemical coprecipitation (Scheme 1d). Due to the fast chemical and electrochemical reactions, the binary metal hydroxides or oxides colloids were in situ formed within the matrix of carbon black and binder. The as-formed electrode configuration with binary colloids in the matrix of carbon and binder can shorten the transfer length of active cations and electrons, leading to the enhancement of electrochemical performance. At the same time, Faradaic redox reaction performed at the binary  $A_xB_{1-x}$  electrode, which can produce pseudocapacitance (Scheme 1e). Because of their colloidal state and electric field assisted activation, the in situ formed binary metal oxides or hydroxides can show high electroactivity during the charging and discharging processes. Our designed binary  $A_xB_{1-x}$  salt electrode may be expected to have the following advantages: (1) both of these raw materials having their own high redox electroactivity and being combined to increase the value of specific capacitance, (2) creating the short ion diffusion paths to enable the fast and reversible Faradaic reactions due to the in-situ formation of electroactive colloid media, (3) these two kinds of metal salts can balance their own crystallization processes during hydrolysis in KOH electrolyte.

Fig. 1 shows the electrochemical performance of  $Fe_xCo_{1-x}$  ( $0 \leq x \leq 1$ ) salt electrodes in 2 M KOH electrolyte, where the molecular ratio ( $x$ ) of between  $Fe^{3+}$  and  $Co^{2+}$  cations is calculated according to the added amount of  $FeCl_3 \cdot 6H_2O$  and  $CoCl_2 \cdot 6H_2O$  salts. Cyclic voltammetry (CV) curves (current density versus potential) at the current rate of 5 mV/s and the potential range of  $-0.1$  to  $0.45$  V are shown in Fig. 1a. A pair of redox peaks is presented at the CV

curves, showing the pseudocapacitive characteristics. The redox peaks of two cations are overlapped that only form one pair of redox peak. When the  $x$  was increased from 0 to 1, both oxidation and reduction peaks potentials shift to positive direction, while both intensities of oxidation and reduction peaks are increased. The increase in area of the CV curves indicates the enhanced specific capacitance with the increase of  $x$  value meaning that the introduction of Fe cations into  $\text{CoCl}_2$  electrode can increase the electrochemical performance of unitary inorganic salt electrode. Therefore, these two cations show synergetic effect on the enhanced capacitance of binary  $\text{Fe}_x\text{Co}_{1-x}$  salt electrode. In the  $\text{Fe}_x\text{Co}_{1-x}$  salt pseudocapacitors, two kinds of Faradaic redox reactions can occur as following:



Therefore, the binary salt electrode can introduce two kinds of redox reactions to increase the value of specific capacitance in our designed ionic pseudocapacitors.

Fig. 1b shows the charge-discharge curves (time versus potential) of  $\text{Fe}_x\text{Co}_{1-x}$  ( $0 \leq x \leq 1$ ) binary salt electrodes measured at the current density of 3 A/g. The outlines of the charge-discharge curves are changed with different  $x$  values in the binary  $\text{Fe}_x\text{Co}_{1-x}$  salt electrode. As shown in Fig. 1b and 1c, the significant charge-discharge plateau can be found with  $x$  value larger than 0.5. The specific capacitance of our designed binary salt pseudocapacitor system can be calculated from the galvanostatic charge-discharge curves according to the following equation:<sup>18</sup>

$$S_c = I\Delta t/m\Delta V \quad (3)$$

where  $I(\text{A})$  is the current used for charge-discharge testing,  $\Delta t(\text{s})$  is the discharge time,  $m(\text{g})$  is the weight of the electroactive transitional metal cations, and  $\Delta V$  is the voltage interval of the discharge process. Variation of specific capacitance as a function of ratio of  $x$  ( $0 \leq x \leq 1$ ) at the current density of 3 A/g is shown in Fig. 1d. The specific capacitance is increased with

the increase of the adding amount of  $\text{Fe}^{3+}$  in binary salt electrode, indicated the  $\text{Fe}^{3+}$  having higher electrochemical activity than that of  $\text{Co}^{2+}$  in our designed inorganic salt pseudocapacitors.

The traditional specific capacitance of a supercapacitor is calculated according to the weight of the active materials, such as the weight of  $\text{Fe}_2\text{O}_3$  or  $\text{Co}(\text{OH})_2$  materials. The pseudocapacitive behavior is associated with primarily to the redox reaction of cations in electrode materials during operation.<sup>1</sup> Based on the physical origin of pseudocapacitors, the specific capacitance calculated from cations can more deeply reflect their real redox mechanism and cation utilization ratio in electrochemical reaction, for example, we can judge the occurrence of one-electron, or two-electron redox reactions by comparing the calculated and measured ionic capacitances. In addition, in our designed binary salt electrode system, inorganic salts with free cations were directly used in fabricating electrodes, thus, the use of specific capacitance of cations herein can more properly evaluate the performance of binary salt pseudocapacitors.

For studying the synergetic role of  $\text{Co}^{2+}$  and  $\text{Fe}^{3+}$  cations, the specific capacitances of individual  $\text{FeCl}_3$  ( $C_{\text{Fe}} = 6166 \text{ F/g}$ ) and  $\text{CoCl}_2$  ( $C_{\text{Co}} = 1429 \text{ F/g}$ ) electrodes were measured and to compare with that of binary cations electrodes. With  $0.1 \leq x \leq 0.9$ , the reference calculated capacitance ( $C_{\text{R}}$ ) values are calculated from the equation,  $C_{\text{R}} = xC_{\text{Fe}} + (1-x)C_{\text{Co}}$ . Fig. 1d shows the measured specific capacitances and reference calculated values. The measured specific capacitances are higher than the reference calculated values at  $0.1 \leq x \leq 0.9$ , confirmed that the specific capacitance of the  $\text{Fe}_x\text{Co}_{1-x}$  salt electrodes is higher than the total value of unitary  $\text{Fe}^{3+}$  and  $\text{Co}^{2+}$  cations. The binary electroactive cations,  $\text{Fe}^{3+}$  and  $\text{Co}^{2+}$ , can significantly enhance their electrochemical performance.  $\text{Fe}_{0.7}\text{Co}_{0.3}$  electrode displays the highest value of  $11789 \text{ F/g}$  at the potential interval of  $0.38\text{V}$  and the current density of  $3 \text{ A/g}$ . The specific capacitances of  $\text{Fe}_{0.6}\text{Co}_{0.4}$  and  $\text{Fe}_{0.8}\text{Co}_{0.2}$  electrodes are  $6375 \text{ F/g}$  and  $8793 \text{ F/g}$ , respectively, which is higher than the reference value from the sum of the values of two individual

component electrodes (Fig. 1d). Fig. S1 shows cycling stability of binary  $\text{Fe}_{0.7}\text{Co}_{0.3}$  electrode measured in 2M KOH electrolyte at the high current density of 10 A/g and at potential interval of 0-0.38 V. The enhanced electrochemical performance of binary  $\text{A}_x\text{B}_{1-x}$  salt pseudocapacitors can be ascribing to the following reason: (1) the electroactive cations of  $\text{Fe}^{3+}$  and  $\text{Co}^{2+}$  were combined to provide two redox reactions; (2) metal cations can be fully utilized in the highly electroactive binary  $\text{A}_x\text{B}_{1-x}$  salt pseudocapacitors, while metal cations only on the surface of active materials can be utilized for charge storage in traditional electrode materials.

The transitional metal oxides like manganese oxide, nickel oxide, iron oxide, cobalt oxide, have been demonstrated as the electrode materials for pseudocapacitors because of their variant oxidation states for efficient redox charge transfer.<sup>19-21</sup> However, the reported values are still far below than their theoretical specific capacitance values (Table 1).<sup>22-27</sup> The theoretical specific capacitance is calculated from the full utilization of cations in electrode materials as the oxidation state of these metal ions is changed from +2 to +3/+4 over a given potential window. In order to highly effectively utilize the reactive cations during the proposed redox reactions, chemists made many efforts to focus on the existing status of active cations. The use of ionic-state active electrode materials is the most promising to fully utilize the redox storage ability of active cation.<sup>28,29</sup> The present results prove that the designed binary composite electrode can solve these problems. As shown in Table 1,  $\text{Fe}_{0.7}\text{Co}_{0.3}$  electrode shows the highest capacitance among the reported values of various pseudocapacitive materials. Different from the reported electrode materials synthesized by the traditional method, our designed highly active materials were in situ formed by electric field assisted chemical coprecipitation. When the pristine binary salt electrodes were contacted with KOH electrolyte, metal cations of  $\text{Co}^{2+}$  and  $\text{Fe}^{3+}$ , immediately reacted with  $\text{OH}^-$  to form electroactive hydroxides or oxides; simultaneously, the external electric field was in situ activating the as-formed hydroxides.

To find the mechanism of high charge storage ability, we studied the compositions and microstructures of the binary salt electrode after electrochemical measurement in KOH electrolyte. Fig. 2 shows XRD patterns of  $\text{Fe}_x\text{Co}_{1-x}$  ( $0 \leq x \leq 1$ ) salt electrodes after electrochemical measurement.  $\text{Fe}_2\text{O}_3$ ,  $\text{Fe}(\text{OH})_3$ , and  $\text{Co}_2\text{O}_3$  phases can be found in XRD patterns, which are consistent with the standard PDF No. 81-2022 for  $\text{Fe}(\text{OH})_3$ , No. 40-1139 for  $\text{Fe}_2\text{O}_3$ , and No. 2-770 for  $\text{Co}_2\text{O}_3$ . As shown in Fig.2, the final phases of binary electrodes can be changed with different  $x$  values. The presence of weak peaks in XRD pattern indicates the formation of poor crystalline colloidal media. We consider the highly electroactive colloids formed by electric field assisted coprecipitation, can be fully utilized in electrochemical Faradaic redox reaction, leading to higher specific capacitance. Very recently, the similar electrode materials have been reported that the amorphous materials can show higher electrochemical performance than that crystallized materials.<sup>30</sup> In binary salts reaction system, the presence of  $\text{Fe}^{3+}$  and  $\text{Co}^{2+}$  cations can affect or disturb the crystallization process of electrode materials, thus, only poor crystalline  $\text{Fe}_2\text{O}_3$ ,  $\text{Fe}(\text{OH})_3$ , and  $\text{Co}_2\text{O}_3$  colloids can be formed under the external electric field.

Fig. 3a-k shows the SEM images of  $\text{Fe}_x\text{Co}_{1-x}$  ( $0 \leq x \leq 1$ ) salt electrodes after electrochemical measurement in 2 M KOH electrolyte. When  $x < 0.5$ , only sheet-like cobalt oxide can be found. With the increase of  $x$  value to 1.0, the sheet-like structures were transformed into particles. After electrochemical reaction, active colloids were formed within the matrix of carbon black and PVDF binder to form new electrode configuration (Scheme 1b). The present results prove that the electroactive colloids were not well crystalline state, but can show highly reactivity toward Faradaic reaction. In addition, the formation of the specific configuration can create short ion diffusion paths to enable the fast and reversible Faradaic reactions.<sup>31,32</sup>

To prove the generality of binary salt electrodes, we studied the electrochemical performances of  $\text{Ni}_x\text{Co}_{1-x}$ ,  $\text{Ni}_x\text{Fe}_{1-x}$ ,  $\text{Co}_x\text{Mn}_{1-x}$ ,  $\text{Fe}_x\text{Mn}_{1-x}$ , and  $\text{Ni}_x\text{Mn}_{1-x}$  salt electrodes in KOH

electrolyte (Figs. S2-S6). We deeply studied the chemical behaviors of two kinds of metal ions in alkaline solution in one binary salt electrode. The chemical roles of Mn(II), Fe(III), Ni(II) and Co(II) ions in mixed solution have been studied by researchers in analytical and environmental field.<sup>33-36</sup> However, it is rare to report the electrochemical performance of these metal cations in one system. As shown in Figs. S2-S6, all of binary salts electrodes can show high electrochemical reactivity toward Faradaic redox reaction. Redox peaks are present at the CV curves, showing the occurrence of pseudocapacitive reaction. When the x values are increased from 0 to 1, both oxidation and reduction peak potentials are shifted. According to CV and discharge curves, the increase of x value can enhance the specific capacitance of binary salt electrodes. It should be noted that the potential interval can reach as large as 1.0 V with the introduction of Mn cations, which can increase the energy density of pseudocapacitors. Figs. S7-S9 shows XRD patterns of  $\text{Ni}_x\text{Co}_{1-x}$ ,  $\text{Ni}_x\text{Fe}_{1-x}$ ,  $\text{Co}_x\text{Mn}_{1-x}$ ,  $\text{Fe}_x\text{Mn}_{1-x}$ , and  $\text{Ni}_x\text{Mn}_{1-x}$  salt electrodes after electrochemical measurement in KOH electrolyte. The weak peaks indicate the formation of poor crystalline colloids formed by electric field assisted chemical coprecipitation.<sup>37-40</sup> Fig. S10 shows SEM images of  $\text{Ni}_x\text{Co}_{1-x}$  salt electrodes after electrochemical measurement in 2 M KOH electrolyte. With the increase of x values, the sheet-like cobalt oxide structures were transformed into particles. The crystallization process was suppressed with adding Ni cations, and these binary salt electrodes can form highly reactive colloids toward Faradaic reaction. These results give a clear indication that the combinatorial transition-metal cation pseudocapacitors can improve the electrochemical performance of inorganic pseudocapacitors.

In summary, we proposed a new combinatorial binary cations pseudocapacitor by an in situ chemical coprecipitation under electric field. Aqueous cation pseudocapacitors with binary  $\text{A}_x\text{B}_{1-x}$  salt electrodes in KOH electrolyte were designed, involving manganese, iron, cobalt, and nickel cations. Starting from these binary  $\text{A}_x\text{B}_{1-x}$  salts, reactive colloids were crystallized via chemical coprecipitation together with Faradaic reactions under electric field, which were

firmly absorbed by carbon black and PVDF matrix. These colloids were confirmed as highly electroactive oxides/hydroxides with high specific capacitance values, which warrant a big promise for finding high-performance electrical energy storage systems. This binary salt pseudocapacitor system is expected to benefit from the major advantages of multiple redox cations, which can provide multiple redox sites to enhance electrochemical performances.

### Acknowledgements

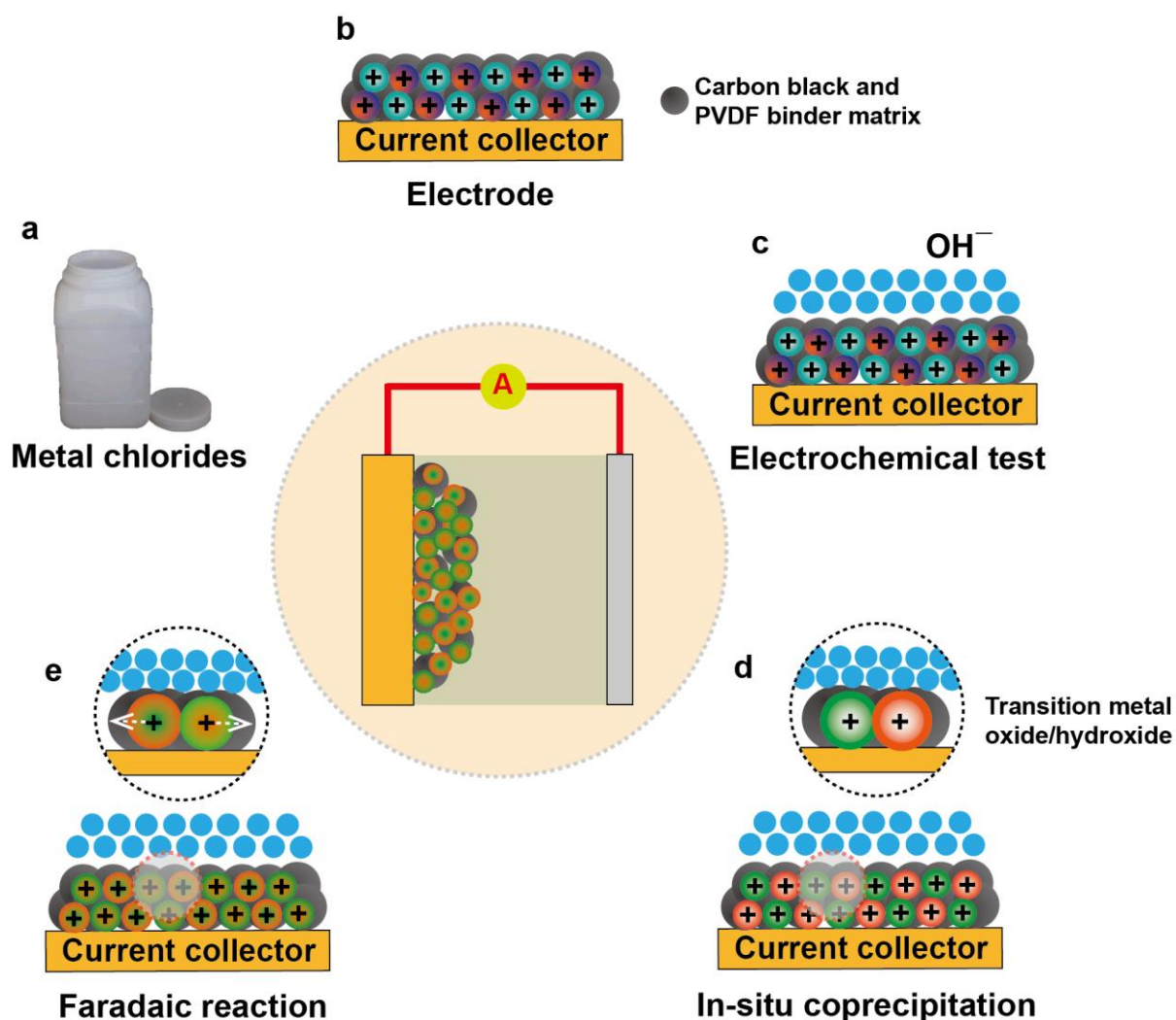
Financial support from the National Natural Science Foundation of China (grant no. 51125009) and National Natural Science Foundation for Creative Research Group (grant no. 21221061), and Hundred Talents Program of Chinese Academy of Science is acknowledged.

### References

- 1 B. E. Conway, *Electrochemical Supercapacitors: Scientific Fundamentals and Technological Applications*, Kluwer Academic/Plenum Publishers, New York 1999.
- 2 A. L. M. Reddy, S. R. Gowda, M. M. Shaijumon, P. M. Ajayan, *Adv. Mater.*, 2012, **24**, 5045-5064.
- 3 Z. Yu, B. Duong, D. Abbitt, J. Thomas, *Adv. Mater.*, 2013, **25**, 3302-3306.
- 4 H. Zhang, X. Yu, P. V. Braun, *Nat. Nanotechnol.*, 2011, **6**, 277-281.
- 5 W. Wang, S. Guo, K. N. Bozhilov, D. Yan, M. Ozkan, C. S. Ozkan, *Small*, 2013, **9**, 3714-3721.
- 6 V. Augustyn, J. Come, M. A. Lowe, J. W. Kim, P. L. Taberna, H. D. Abruna, P. Simon, B. Dunn, *Nat. Mater.*, 2013, **12**, 518-522.
- 7 F. Liu, S. Song, D. Xue, H. Zhang, *Adv. Mater.*, 2012, **24**, 1089-1094.
- 8 X. Zhao, B. M. Sanchez, P. J. Dobson, P. S. Grant, *Nanoscale*, 2011, **3**, 839-855.
- 9 V. Augustyn, P. Simon, B. Dunn, *Energy Environ. Sci.*, 2014, **7**, 1597-1614.
- 10 J. Liu, H. Xia, D. Xue, L. Lu, *J. Am. Chem. Soc.*, 2009, **131**, 12086-12087.

- 11 K. Zaghbi, A. Mauger, H. Groult, J. B. Goodenough, C. M. Julien, *Mater.*, 2013, **6**, 1028–1049.
- 12 K. Chen, Y. D. Noh, K. Li, S. Komarneni, D. Xue, *J. Phys. Chem. C*, 2013, **117**, 10770–10779.
- 13 D. Sarkar, G. G. Khan, A. K. Singh, K. Mandal, *J. Phys. Chem. C*, 2013, **117**, 15523–15531.
- 14 F. Liu, D. Xue, *Chem. Eur. J.*, 2013, **19**, 10716–10722.
- 15 M. Song, S. Cheng, H. Chen, W. Qin, K. Nam, S. Xu, X. Yang, A. Bongiorno, J. Lee, J. Bai, T. A. Tyson, J. Cho, M. Liu, *Nano Lett.*, 2012, **12**, 3483–3490.
- 16 R. Wang, X. Yan, *Sci Rep.*, 2014, **4**, 3712.
- 17 J. Liu, J. Jiang, C. Cheng, H. Li, J. Zhang, H. Gong, H. J. Fan, *Adv. Mater.*, 2011, **23**, 2076–2081.
- 18 H. Wang, Q. Gao, J. Hu, *J. Power Sources*, 2010, **195**, 3017–3024.
- 19 I. E. Rauda, V. Augustyn, B. Dunn, S. H. Tolbert, *Acc. Chem. Res.*, 2013, **46**, 1113–1124.
- 20 P. Simon, Y. Gogotsi, *Nat. Mater.*, 2008, **7**, 845–854.
- 21 P. Lu, F. Liu, D. Xue, H. Yang, Y. Liu, *Electrochim. Acta*, 2012, **78**, 1–10.
- 22 W. Yang, Z. Gao, J. Ma, J. Wang, B. Wang, L. Liu, *Electrochim. Acta*, 2013, **112**, 378–385.
- 23 Xue T, Lee J, *J. Power Sources*, 2014, **245**, 194–202.
- 24 M. Zhu, Y. Wang, D. Meng, X. Qin, G. Diao, *J. Phys. Chem. C*, 2012, **116**, 16276–16285.
- 25 G. Lee, Y. Cheng, C. V. Varanasi, J. Liu, *J. Phys. Chem. C*, 2014, **118**, 2281–2286.
- 26 G. Yang, C. Xu, H. Li, *Chem. Commun.*, 2008, **48**, 6537–6539.
- 27 X. Lang, A. Hirata, T. Fujita, M. W. Chen, *Nat. Nanotechnol.*, 2011, **6**, 232–236.
- 28 K. Chen, D. Xue, *Colloids Interface Sci. Commun.*, 2014, **1**, 39–42.
- 29 K. Chen, D. Xue, *J. Colloid Interface Sci.*, 2014, **416**, 265–271.
- 30 K. Chen, S. Song, D. Xue, *RSC Adv.*, 2014, **4**, 23338–23343.

- 31 R. B. Rakhi, W. Chen, M. N. Hedhili, D. Cha, H. N. Alshareef, *ACS Appl. Mater. Interfaces*, 2014, **6**, 4196-4206.
- 32 I. Shakir, Z. Ali, J. Bae, J. Park, D. J. Kang, *Nanoscale*, 2014, **6**, 4125-4130.
- 33 A. Duran, M. Tuzen, M. Soylak, *J. Hazard. Mater.*, 2009, **169**, 466-471.
- 34 M. Tuzen, K. O. Saygi, C. Usta, M. Soylak, *Bioresource Technol.*, 2008, **99**, 1563-1570.
- 35 M. Tuzen, K. O. Saygi, M. Soylak, *J. Hazard. Mater.*, 2008, **152**, 632-639.
- 36 M. Tuzen, M. Soylak, *J. Hazard. Mater.*, 2007, **147**, 219-225.
- 37 K. Chen, D. Xue, *J. Colloid Interface Sci.*, 2014, **424**, 84-89.
- 38 K. Chen, S. Song, K. Li, D. Xue, *CrystEngComm*, 2013, **15**, 10367-10373.
- 39 K. Chen, Y. Yang, K. Li, Z. Ma, Y. Zhou, D. Xue, *ACS Sustainable Chem. Eng.*, 2014, **2**, 440-444.
- 40 K. Chen, F. Liu, D. Xue, S. Komarneni, *Nanoscale*, 2014, DOI: 10.1039/C4NR05919K.



**Scheme 1.** Schematic drawing of in-situ formation of the combinatorial transition-metal cations pseudocapacitor. (a,b) The fabrication of electrode by slurry-coating manufacturing. A commercial transition metal chlorides salts/carbon black-binder mixture (slurry) is pasted onto the current collector for the fabrication of electrode, which did not need complex synthesis procedure. When the as-prepared electrode is immersed into KOH electrolyte (c), transition metal cations immediately transform into metal hydroxides or oxides by electric field assisted chemical coprecipitation (d). In-situ synthesized transition metal oxide/hydroxide subsequently integrated into practical electrode structures. (e) At the same time, pseudocapacitive Faradaic reaction was occurred at the same electrode. In-situ synthesized transition metal oxide/hydroxide can enhance electrochemical utilization of active metal cations.

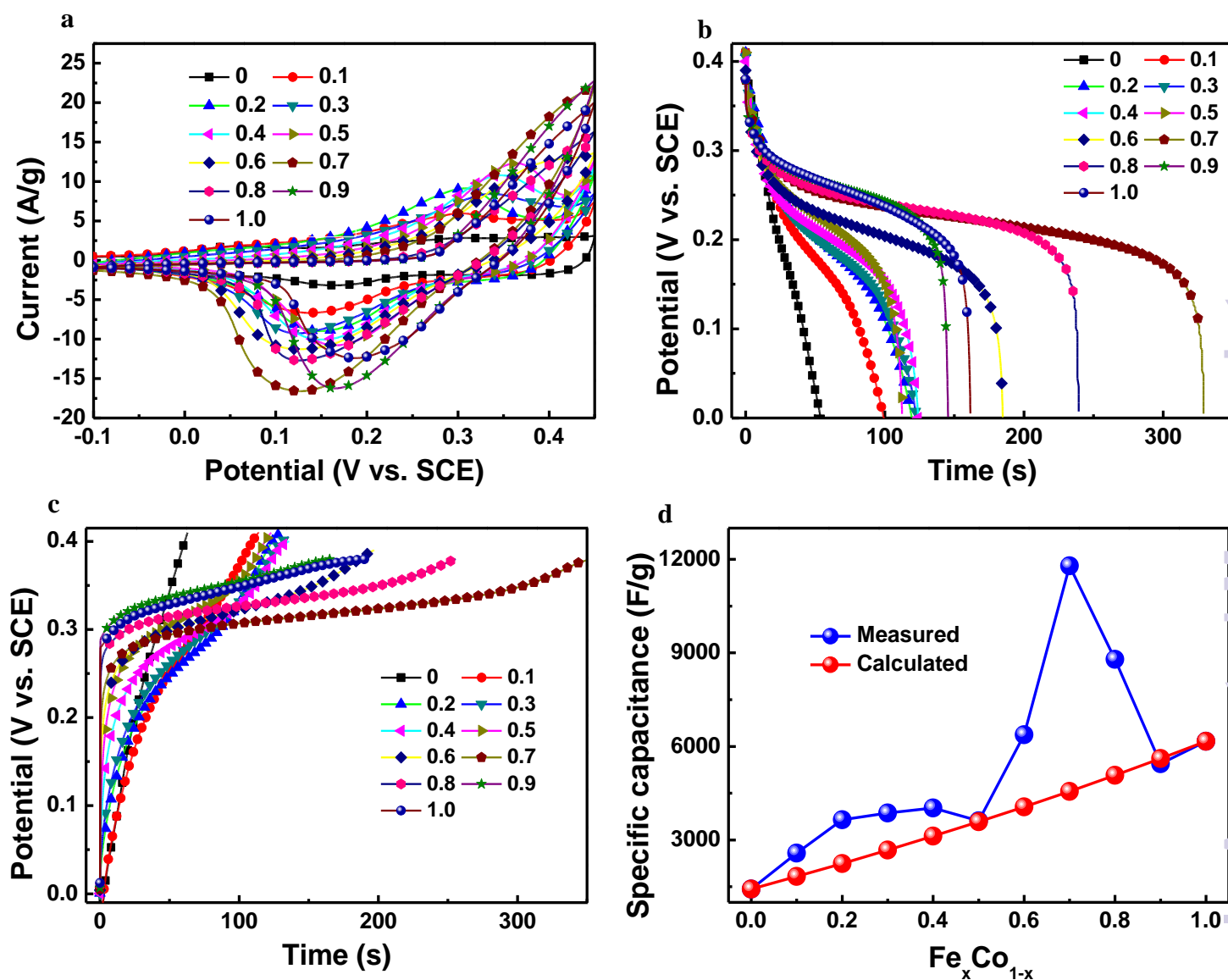


**Fig. 1.** Electrochemical performance of  $\text{Fe}_x\text{Co}_{1-x}$  ( $0 \leq x \leq 1$ ) salt electrodes in 2 M KOH electrolyte. (a) CV curves (current density versus potential) at scan rate of 5 mV/s and potential range of -0.1-0.45 V. A pair of redox peaks is present at the CV curves, showing the pseudocapacitive characteristic. (b) The discharge and (c) charge curves measured at current density of 3 A/g. (d) Variation of specific capacitance as a function of ratio of  $x$  ( $0 \leq x \leq 1$ ) at current density of 3 A/g. The values of  $x$  are shown in graph.

Table 1 Comparison of the supercapacitor performances of metal oxides/hydroxides

Material	Specific capacitance (F/g)	Electrolyte	Potential range (V)	Theoretical capacitance (F/g)	Ion specific capacitance (F/g)*	Ref.
Co <sub>3</sub> O <sub>4</sub>	1063 (10mA/cm <sup>2</sup> )	6M KOH	0–0.38	4216	4343	22
Co(OH) <sub>2</sub>	1180 (4A/g)	1M KOH	–0.1-0.45	3775	1881	23
α-Fe <sub>2</sub> O <sub>3</sub>	340.5 (1A/g)	1M KOH	–0.1-0.44	2234	976	24
NiO/rGO	1077 (1A/g)	6M KOH	–0.1-0.4	2584	1371	25
Ni(OH) <sub>2</sub> /Ni	3152 (4A/g)	3% KOH	–0.05-0.45	2075	4978	26
MnO <sub>2</sub> /Au	1145 (50mV/s)	2 M Li <sub>2</sub> SO <sub>4</sub>	0-0.8	1553	1812	27
Ni-Co oxide	1846 (1A/g)	2M KOH	0-0.37	--	7559	16
Fe <sub>0.7</sub> Co <sub>0.3</sub>	--(3A/g)	2M KOH	0-0.38V	--	11789	This work

\*Ion specific capacitance is calculated according to equation (3).<sup>28</sup>

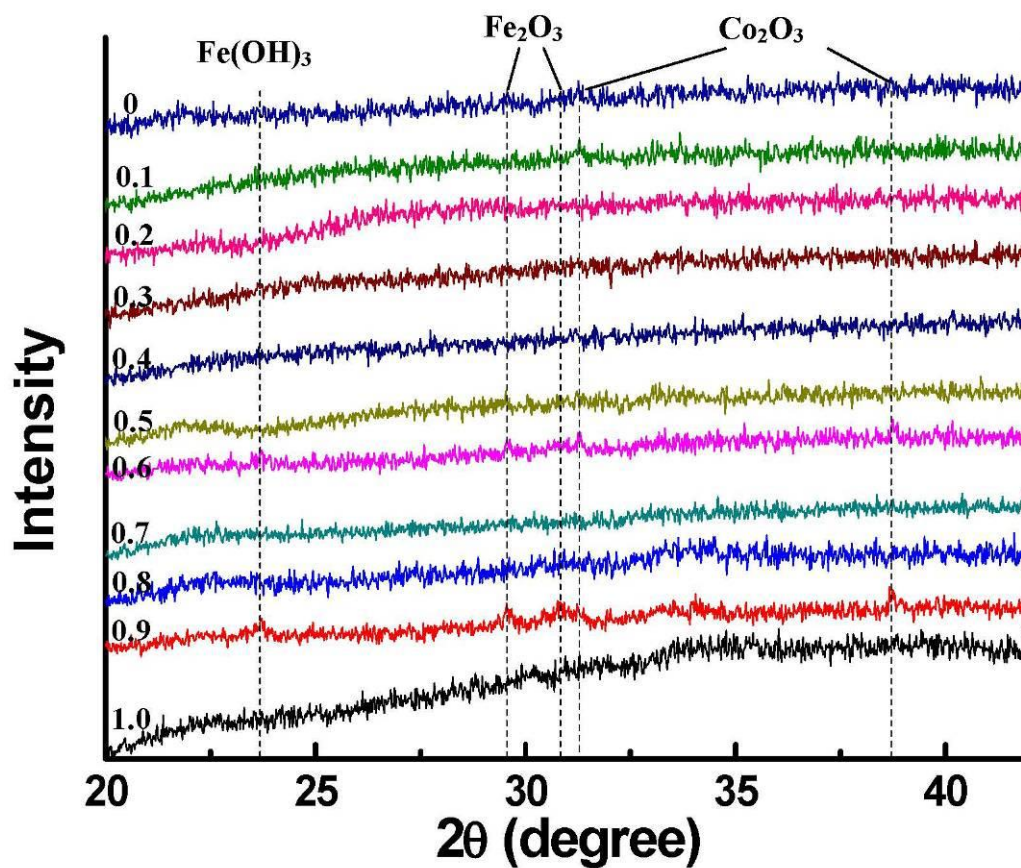


**Fig. 2.** XRD patterns of Fe<sub>x</sub>Co<sub>1-x</sub> ( $0 \leq x \leq 1$ ) salt electrodes after electrochemical measurement in 2 M KOH electrolyte. Fe<sub>2</sub>O<sub>3</sub>, Fe(OH)<sub>3</sub>, and Co<sub>2</sub>O<sub>3</sub> phases are indicated in figure, which are consistent with the standard JCPDS No.81-2022 for Fe(OH)<sub>3</sub>, 40-1139 for Fe<sub>2</sub>O<sub>3</sub>, 2-770 for Co<sub>2</sub>O<sub>3</sub>. The values of x are shown in graph.

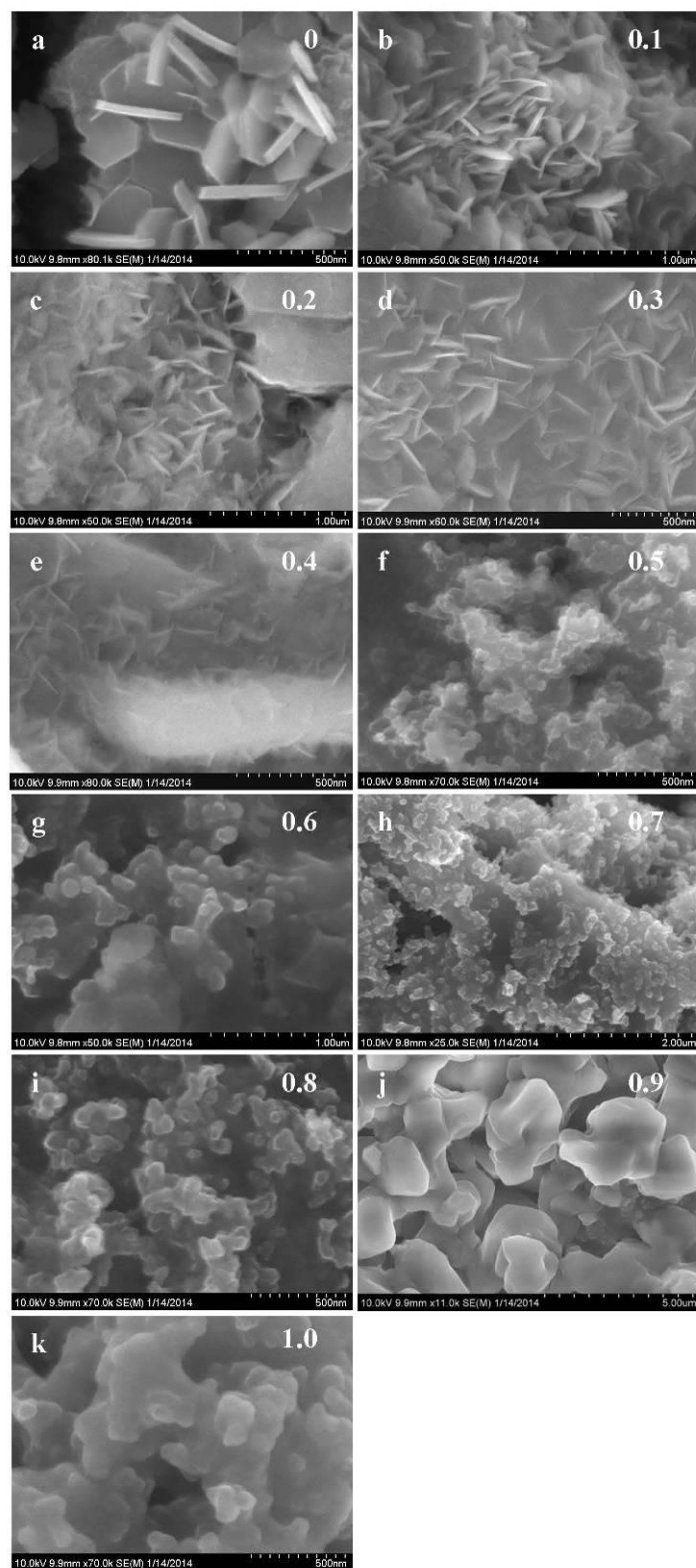


**Fig. 3.** SEM images of  $\text{Fe}_x\text{Co}_{1-x}$  ( $0 \leq x \leq 1$ ) salt electrodes after electrochemical measurement in 2 M KOH electrolyte. With the increase of  $x$  value, the sheet-like structures were transformed into particles. The values of  $x$  are shown in graphs: (a) 0, (b), 0.1, (c) 0.2, (d) 0.3, (e) 0.4, (f) 0.5, (g) 0.6, (h) 0.7, (i) 0.8, (j) 0.9, (k) 1.0.

## TOC

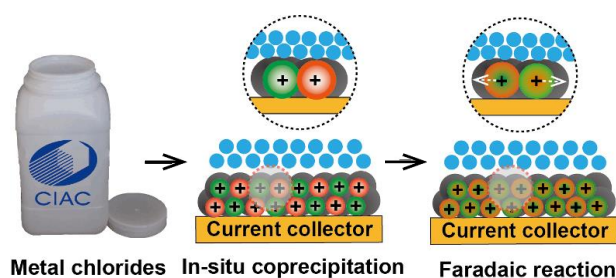
**Binary  $A_xB_{1-x}$  ionic alkaline pseudocapacitor system involving manganese, iron, cobalt, and nickel: formation of electroactive colloids via in-situ electric field assisted coprecipitation**

*Kunfeng Chen<sup>1</sup>, Shu Yin<sup>2,\*</sup> and Dongfeng Xue<sup>1,\*</sup>*

<sup>1</sup>State Key Laboratory of Rare Earth Resource Utilization, Changchun Institute of Applied Chemistry, Chinese Academy of Sciences, Changchun 130022, China

<sup>2</sup>Institute of Multidisciplinary Research for Advanced Materials, Tohoku University, 2-1-1 Katahira, Aoba-ku, Sendai 980-8577, Japan

\*E-mail: shuyin@tagen.tohoku.ac.jp; dongfeng@ciac.ac.cn



Binary  $A_xB_{1-x}$  ionic alkaline pseudocapacitor system involving manganese, iron, cobalt, and nickel were designed via in-situ electric field assisted coprecipitation.